International Journal of Scientific Research in Engineering & Technology
Volume5, Issue2 (March-April 2025), PP: 39-46.
https://www.doi.org/10.59256/ijsreat.20250502007
www.ijsreat.com
ISSN No: 2583-1240

Power Quality Enhancement and Stability Improvement in A Standalone Photovoltaic-Battery Energy Storage System for Reliable Renewable Power Supply

Dharavath Chandrashekar [1], P. Satish Kumar [2]
[1,2] *Department of Electrical Engineering, Osmania University, Hyderabad, Telangana. India.*

To Cite this Article: *Dharavath Chandrashekar [1], P. Satish Kumar [2], "Power Quality Enhancement and Stability Improvement in A Standalone Photovoltaic-Battery Energy Storage System for Reliable Renewable Power Supply", International Journal of Scientific Research in Engineering & Technology, Volume 05, Issue 02, March-April 2025, PP: 39-46.*

Abstract: *In order to satisfy local load demands, this study investigates a stand-alone renewable energy system that consists of a photovoltaic (PV) plant and a battery energy storage system (BES). To improve power extraction efficiency, the PV system makes use of Sliding Mode Control (SMC) in conjunction with Perturb and Observe (P&O) Maximum Power Point Tracking (MPPT). The BES is linked at a common DC bus to ensure system stability and continuous power supply. To improve energy conversion, an anti-windup proportional-integral (AWPI) controller is deployed in the inverter control system for active power regulation and harmonic reduction. This approach significantly minimizes Total Harmonic Distortion (THD) in inverter voltage and current, leading to superior power quality. The effectiveness of the system is confirmed by simulation results, which show improved performance in harmonic mitigation and renewable power consumption. The findings confirm that integrating SMC-based MPPT and AWPI inverter control enhances stability, efficiency, and reliability, making it a viable solution for sustainable power generation.*

Key Word: *MPPT (Maximum Power Point Tracking) and PV (Photo Voltaic) SMC P&O (Sliding Mode Control Perturb and Observe), APC (Active Power Control), AWPI Anti-windup Proportional Integral), Simulink, MATLAB (Matrix Laboratory).*

I.INTRODUCTION

The increased adoption of renewable energy sources is essential for replacing conventional power generation methods. These renewable sources are integrated into the grid using multiple power electronic converters to ensure stable power injection. In some cases, the grid operates as a **microgrid**, supplying power to local loads with a lower power rating. To ensure proper grid integration, renewable sources must be synchronized with the grid frequency, voltage magnitude, and phase angles across all three phases [1].

Grid-connected renewable energy systems are generally stable and less complex due to the presence of an infinite utility grid source. In cases where renewable generation is insufficient due to high load demand, the utility grid compensates for the shortfall. Conversely, when excess renewable energy is produced, the surplus power is injected into the grid to support other loads [2]. This makes grid-connected renewable systems more reliable and efficient for sustained operation.

However, when renewable sources operate in standalone mode**,** they lack grid support, posing stability challenges due to their variable nature. Since renewable energy generation depends on environmental conditions, direct connection to loads is impractical. To mitigate this issue, Battery Energy Storage Systems (BES**)** are employed to store excess energy and supply power during low-generation periods. The BES module is integrated at the DC link**,** where both renewable sources and loads are connected, ensuring voltage stability. This study analyzes a standalone system utilizing photovoltaic (PV) and wind energy sources**,** integrated with BES to effectively supply local loads [3].

II. PV RENEWABLE GENERATION SYSTEM

The standalone renewable system's general architecture, shown in Figure 1, includes a separate DC/DC converter for the PV array. The BES is connected to the DC bus directly for power exchange. These DC/DC convertersof the renewable modules ensure maximum power extraction from PV array. At the DC bus a central inverter and control is connected which converts DC powerfrom the renewable and battery modules to AC [4]. The converted AC is fed to residential and dump loads with controlled voltage and frequency controller.

the DC/DC converters are controlled by individual SMC P&O MPPT gettingfeedback signals from source voltage and current (V_{pv} and I_{pv}). The central inverter is controlledbyAPC based AWPI control module with feedback signals from 3-ph load voltages and currents (V_{Labc} and I_{Labc}). The SMC P&O MPPT is l updated to sliding mode control MPPT for increased power extraction from the renewable sources.The interfacing inverter controller is integrated with AWPI controller for reduced disturbances in the reference signals[5]. As a result, the AC side of the inverter that is linked to the load has less harmonics.

In this paper the standalone renewable source system outline diagram is discussed in section 1which includes the description

of PV modules. The next section 2 has the circuit configuration of each module of the proposed renewable standalone system. Section 3 discusses the construction of controllers for circuit topologies that incorporate feedback from numerous signals. Section 4 presents the simulation and result analysis using several suggested controllers, together with all graphical figures verifying the concept. The final section 5 has the conclusion andreferences of the paper determining the optimal controller for the standalone renewable system.

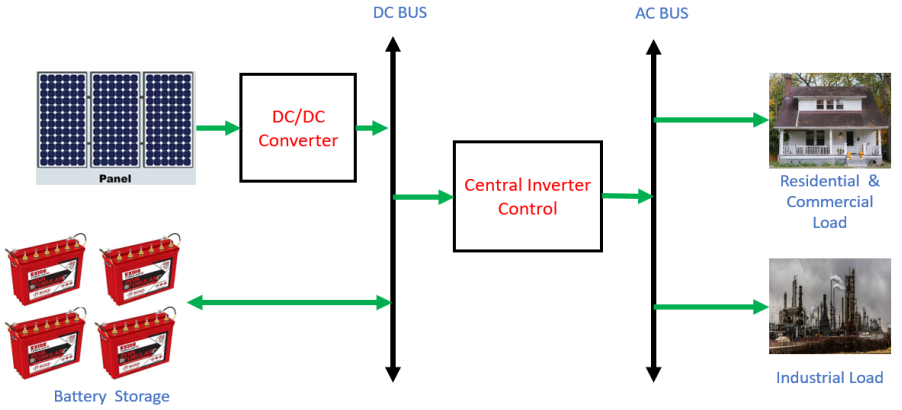

Figure 1: PV Renewable Generation System

III. PROPOSED ADVANCED CONTROLLER FOR PV RENEWABLE GENERATION SYSTEM

As mentioned in Section 1**,** the proposed standalone renewable energy system integrates two renewable sources, primarily a photovoltaic (PV) module**.** To ensure DC voltage stability**, a** battery energy storage system (BES**)** is connected at the DC link [6]. The PV module consists of multiple PV panels arranged in series and parallel to achieve the required voltage and current levels. A DC-DC converter is necessary to improve and control the voltage prior to system integration since PV panels provide DC electricity. Figure 2 depicts the entire system structure, which includes the BES module, power electronics components, and renewable sources that aid in stabilizing and supplying power to the associated load.

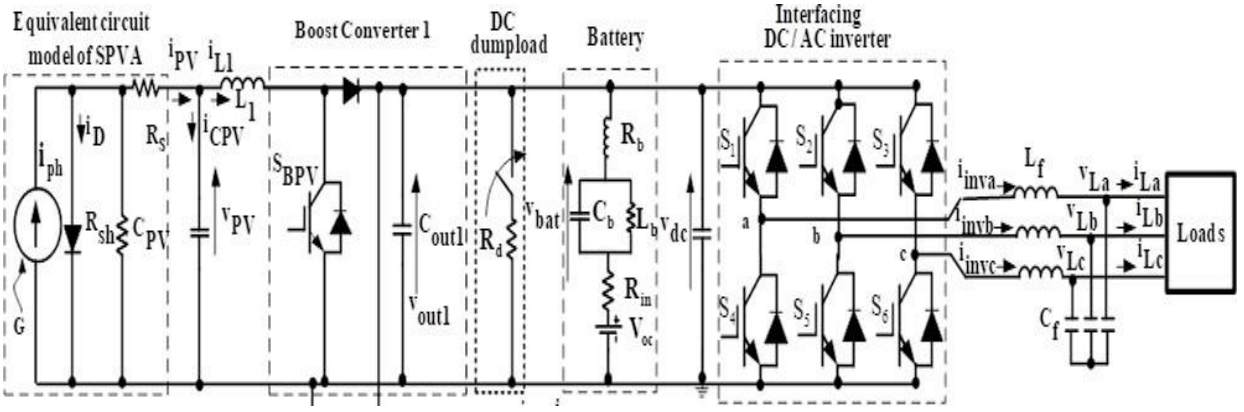

Figure 2: Circuit structure of standalone renewable source system

As illustrated in Figure 2, the PV module is integrated with DC-DC boost converters**,** each equipped with a single power IGBT switch**.** An LC filter, which is based on the switching frequency and maximum load capacity, is positioned between the inverter and load in order to reduce harmonic distortion. **[7].** The system employs three separate controllers to regulate the renewable power circuits and inverter operation. The PV module controller follows a similar structure, with only variations in the input signals. Meanwhile, the inverter controller utilizes feedback signals from the load side to ensure proper regulation. A detailed design of the proposed controllers, along with their mathematical expressions, is provided in the following sections [8].

IV. SLIDING MODE CONTROL PERTURB AND OBSERVE MPPT (SMC P&O MPPT)

In most of the conventional MPPT techniques the P&O method is commonly used for maximum power extraction from the renewable sources. Any MPPT method needs input voltage (V_{pv}) and input current (I_{pv}) as reference signals for the generation of either reference voltage (V_{ref}) or duty ratio (D) [9]. With faster response to input signals, the MPPT method is considered better. This study integrates a "modified P&O MPPT" approach with SMC to manage the DC/DC boost converter's IGBT switch. The control structure of the SMC P&O MPPT module, which generates the duty ratio, is shown in Figure 3.

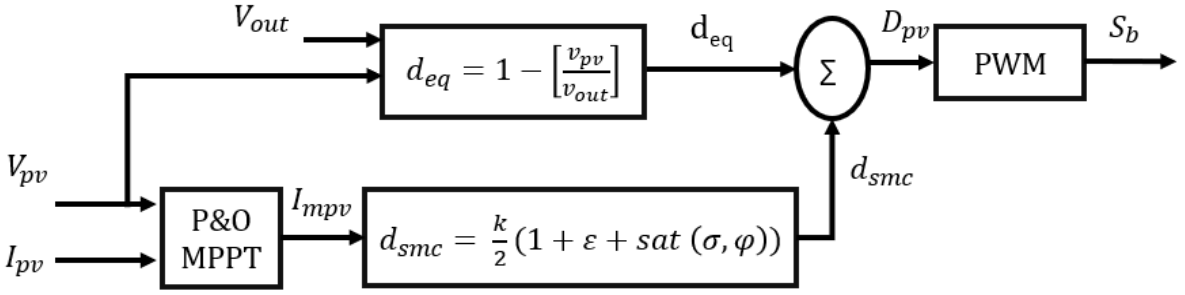

Figure 3: SMC P&O MPPT structure

As per the given structure the final duty ratio (D_{pv}) is addition of two duty ratio factors d_{eq} and d_{smc} which are generated by multiple variables [10]. The final duty ratio (D_{pv}) is given as:

$$D_{pv} = d_{eq} + d_{smc} \quad (1)$$

$$d_{eq} = 1 - \left[\frac{v_{pv}}{v_{out}}\right] \quad (2)$$

$$d_{smc} = \frac{k}{2}(1 + \varepsilon + sat\,(\sigma, \varphi)) \quad (3)$$

The input and output voltages of the DC/DC boost converter are denoted by v_{pv} and v_{out}, respectively, in expressions (2) and (3). These vriables determine the duty factor d_{eq}, where as the d_{smc} duty factor is determined by variables 'k' and 'ε' which are controller gain and error coefficient respectively [11]. The $sat\,(\sigma, \varphi)$ is determined as:

$$sat\,(\sigma, \varphi) = \begin{cases} 1\ if\ \sigma > \varphi \\ \frac{\sigma}{\varphi}\ if\ |\sigma| \leq \varphi \\ -1\ if\ \sigma < \varphi \end{cases} \quad (4)$$

Here, φ is the sliding layer value considered between -0.5 to 0.5. And the σ is calculated as:

$$\sigma = v_{pv} + i_{mpv}\left(\frac{dv_{pv}}{di_{mpv}}\right) \quad (5)$$

$$i_{mpv} = i_{mpv}(t-1) + \nabla D_{pv} \begin{Bmatrix} If\ P(t) > P(t-1)\ and\ V(t) > V(t-1) \\ If\ P(t) < P(t-1) amd\ V(t) < V(t-1) \end{Bmatrix} \quad (6)$$

$$i_{mpv} = i_{mpv}(t-1) - \nabla D_{pv} \begin{Bmatrix} If\ P(t) < P(t-1)\ and\ V(t) > V(t-1) \\ If\ P(t) > P(t-1) amd\ V(t) < V(t-1) \end{Bmatrix} \quad (7)$$

Here, $i_{mpv}(t-1)$ is the previous value of i_{mpv}, ∇D_{pv} is the updated variable to the i_{mpv} either increasing or decrease as per conditions. V(t), P(t) and V(t-1), P(t-1) are the present and past values of input voltage and power to the boost converter respectively [12]. These expressions' ultimate duty ratio (D_{pv}) is contrasted with a high frequency triangle waveform that produces a PWM pulse for an IGBT boost converter switch. The maximum power extraction is achieved with sliding control of the duty ratio and the power is fed to DC link. Each converter of the renewable source has individual SMC P&O MPPT technique integrated in each module.

V. ACTIVE POWER CONTROL BASED ANTI-WINDUP PROPORTIONAL INTEGRAL (ANC BASED AWPI CONTROLLER)

The APC base AWPI controller is an advanced technique for controlling the interfacing inverter between the load and DC link. The controller needs load voltage and current signals feedback for stable voltage magnitude and frequency generation [13]. The Figure 4 represents the complete control structure of the proposed APC base AWPI controller with Sinusoidal PWM technique.

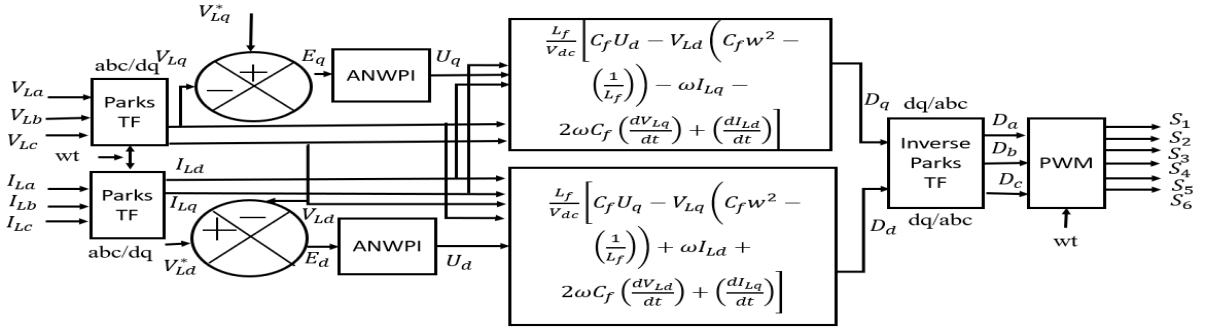

Figure 4: APC base AWPI controller of interfacing inverter module

The reference signals to the Sinusoidal PWM generator are generated by Dq components (D_d and D_q). The controller generates reference signals based on the Dq component of load voltages and currents. The Dq components for VLabc and ILabc are generated using Park's transformation as expressed below.

$$\begin{bmatrix} F_d \\ F_q \end{bmatrix} = \begin{bmatrix} Sin\,\theta & -Cos\,\theta & 0 \\ Cos\,\theta & Sin\,\theta & 0 \end{bmatrix} \begin{bmatrix} F_a \\ F_b \\ F_c \end{bmatrix} \quad (8)$$

Here, 'F' can be any signal either VL or IL and 'θ' is the phase angle of phase A determined by PLL (Phase Lock Loop) block. The PLL is fixed with 50Hz fundamental frequency for the operation of the inverter at specified frequency. From the VL and IL dq components achieved from expression (6) the reference signals D_d and D_q are generated as:

$$D_d = \frac{L_f}{V_{dc}}\left[C_f U_d - V_{Ld}\left(C_f w^2 - \left(\frac{1}{L_f}\right)\right) - \omega I_{Lq} - 2\omega C_f\left(\frac{dV_{Lq}}{dt}\right) + \left(\frac{dI_{Ld}}{dt}\right)\right] \quad (9)$$

$$D_q = \frac{L_f}{V_{dc}}\left[C_f U_q - V_{Lq}\left(C_f w^2 - \left(\frac{1}{L_f}\right)\right) + \omega I_{Ld} + 2\omega C_f\left(\frac{dv_{Ld}}{dt}\right) + \left(\frac{dI_{Lq}}{dt}\right)\right] \quad (10)$$

Here, V_{dc} is the measured DC link voltage, L_f and C_f are the filter inductance and capacitance values, ω is the fixed angular frequency (2.π.50), $\frac{dV_{Ld}}{dt}\frac{dV_{Lq}}{dt}$ and $\frac{dI_{Ld}}{dt}\frac{dI_{Lq}}{dt}$ are the change in Dq VL and IL values. The U_d and U_q components are generated using error dq components fed to AWPI controller [14]. The U_d is generated by error component comparing V_{Ld}^* and V_{Ld}. Similarly, u_q is generated error component comparing V_{Lq}^* and V_{Lq}

$$E_d = V_{Ld}^* - V_{Ld} \quad (11)$$

$$E_q = V_{Lq}^* - V_{Lq} \quad (12)$$

The internal modelling of the AWPI controller with input and output signals is presented in Figure 5.

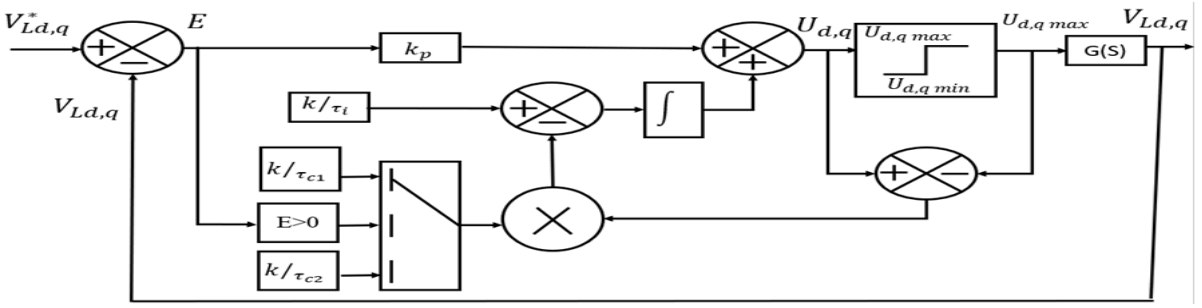

Figure 5: AWPI controller internal structure

Similar to conventional PI controller, the AWPI controller has fixed proportional gain 'k'. The integral gain is varied as per the error signal (E) of Dq voltage components [15]. The U_d and U_q signals are given as:

$$U_d = E_d\left(\frac{k\tau_c(\tau_i s+1)}{\tau_i(\tau_c s+1)}\right) + u_{d\,max}\left(\frac{1}{(\tau_c s+1)}\right) \quad (13)$$

$$U_q = E_q\left(\frac{k\tau_c(\tau_i s+1)}{\tau_i(\tau_c s+1)}\right) + u_{q\,max}\left(\frac{1}{(\tau_c s+1)}\right) \quad (14)$$

Where, τ_i and τ_c are the integral gain coefficients are tuned depend on response of the system. The following section validates the models and simulations of all the circuit topologies and control structures under various operating situations.

VI.RESULTS

The complete modeling of the standalone renewable source system with BES module compensating the local load is done in Simulink environment. The blocks from 'Specialized Power systems' in the library browser are considered for the modeling of the system. Differentblocks from 'Electrical sources', 'Passive elements', 'Power electronics' and 'Commonly UsedBlocks' subsets are imported for the modeling. The parameters of the modules are updated as per the configuration values in table 1 and the simulation is run for different conditions.

Table 1: Configuration values of modules

Name of the module	Parameters
PV module	Manufacturer: SunPower SPR-305E-WHT-D V_{mp} = 54.7V, I_{mp} = 5.58A, V_{oc} = 64.2V, I_{sc} = 5.96A, N_s = 7, N_p = 7, P_{pv} = 14 kW Boost converter: C_{in} =100µF, L_b = 500mH, R_{igbt} = 0.01Ω, $V_{f\,diode}$ = 0.8V

Battery	Lithium Ion 70kWhr: V_{nom} = 760V, Capacity =100Ah,
Inverter	Rigbt = 1mΩ, Lf = 1mH, Cf = 100µF
SMC MPPT	$\Delta D = \pm 1$, MPPT gain = 5, k = 0.017, e = 0.05, φ = -0.5, f_S = 5kHz
Active power control	VLd* = 240Vrms ph, VLq* = 0, Fn = 50Hz,k = 10, r_i = 0.01, r_{c1} = 0.1, r_{c2} = 10, f_S = 5kHz

As per the given parameters in Table 1 the standalone renewable system is updated. The valuesof each passive element of the circuit topologies and the controller gain values are given basedon stability tuning of the system. After updating the parameters, a simulation is carried out using Discrete analysis by 'Tustin' solver type set in 'powergui' block for generation of graphical plots. All the voltages, powers and currents of each module are plotted with simulation time as reference and are given below.

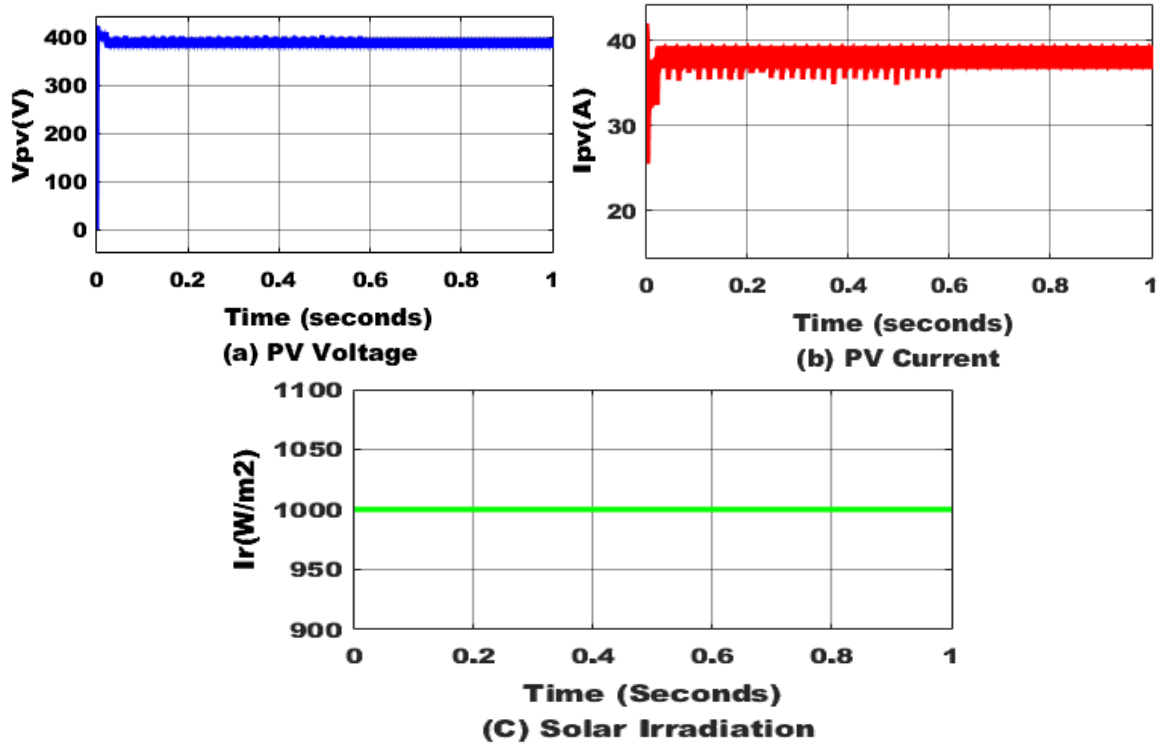

Figure 6: Photo Voltaic array characteristics

The simulation is run for 1sec with constant solar irradiation and wind speed set at 1000W/mt2and 12m/sec throughout the simulation. The Figure 6 shows characteristics of the PV array with 387V V_{pv} and 38A I_{pv}. The total power generated by PV array is 14 kW which is either shared to the load or stored in battery pack as per the power demand.

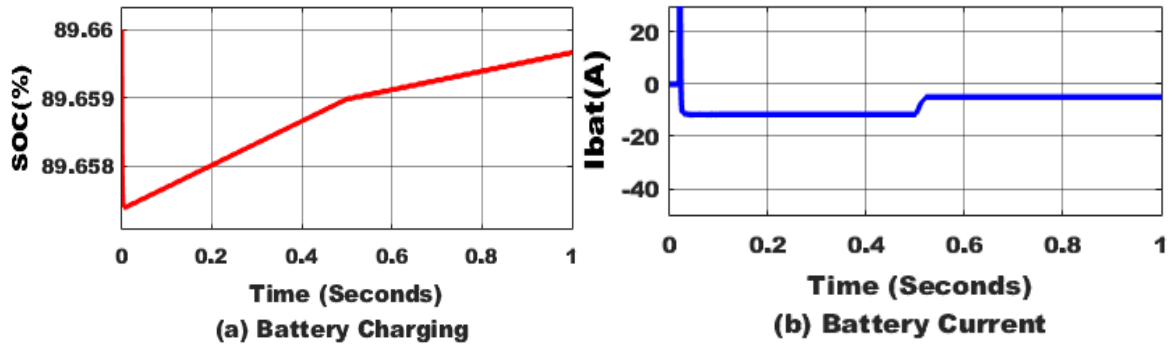

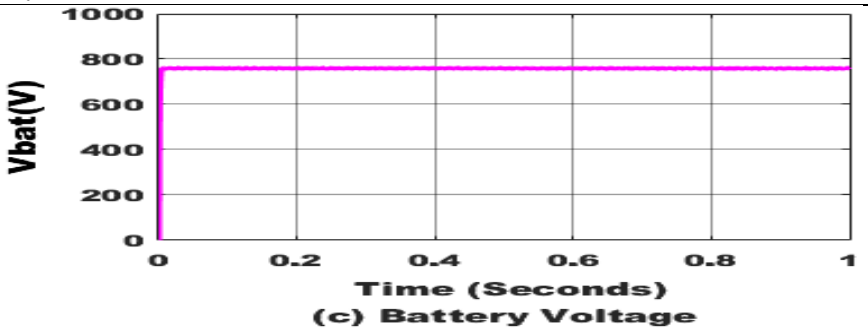

Figure 7: Characteristics of Battery pack

As the battery pack is connected at the DC link, it receives excess power after consumed by the load. The characteristics of the battery pack are presented in Figure 7. The rising of SOCand negative current depicts charging of the battery from the renewable source's powers. The voltage of the battery is recorded at 760V which is the nominal voltage of the battery at 90% initial SOC.

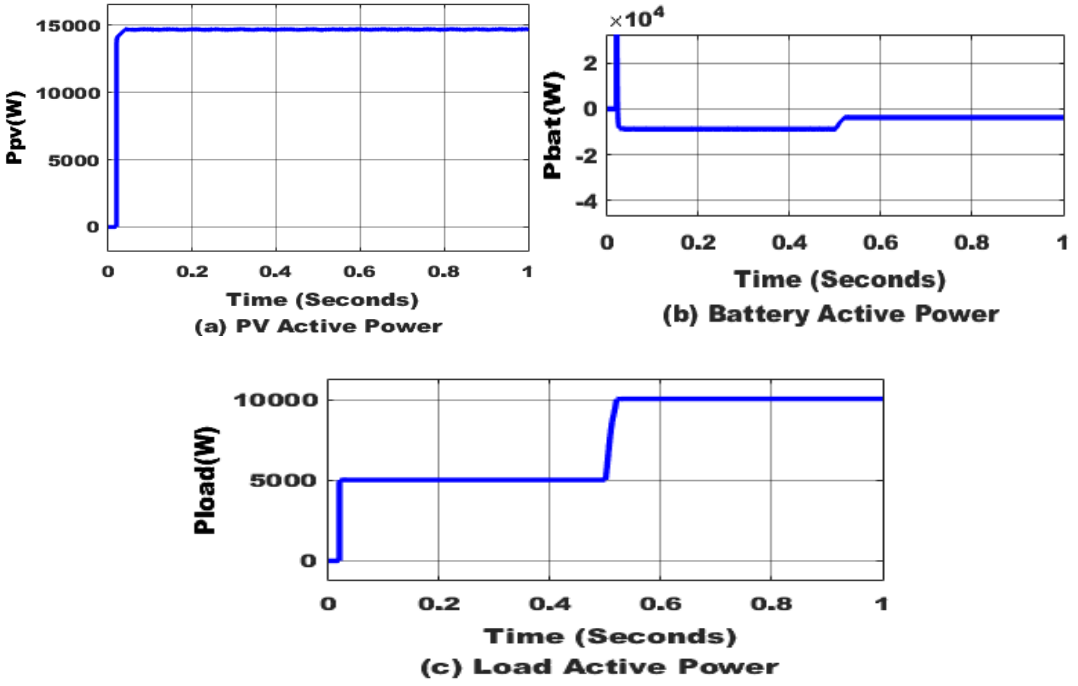

Figure 8: Active Powers of PV, Battery, Load

The Figure 8 has the active powers of the PV source, battery pack and load demand. After the consumption of 14 kW by the load the remaining renewable power of 3 kW isstored in the battery pack represented in negative direction and losess1 kw.

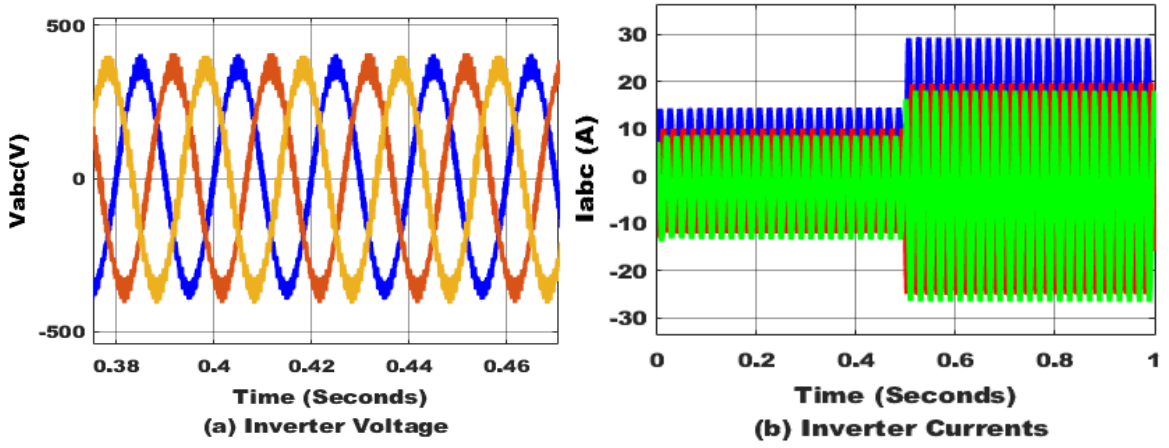

Figure 9: voltages and currents of interfacing inverter

Figure 9 shows the observed three-phase voltages and currents at the inverter's output following the LC filter. Figure 10

displays the active and reactive powers of the electricity supplied by the inverter based on the three phase voltages and currents.

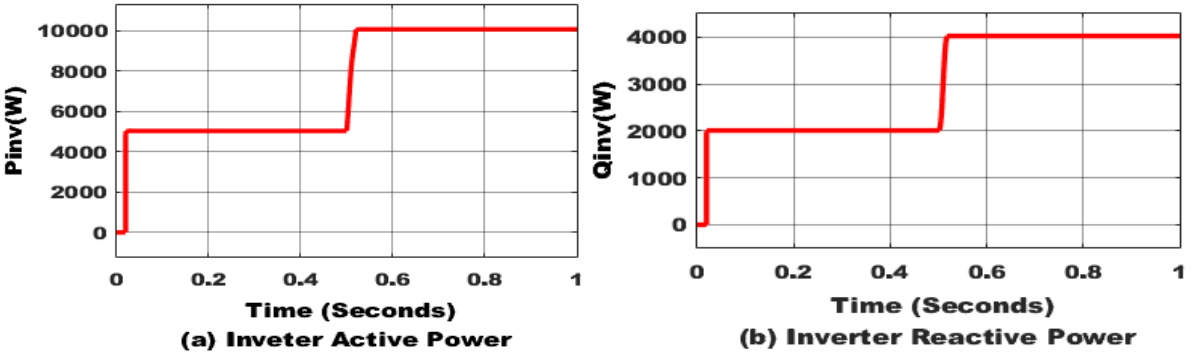

Figure 10: Active (P) and Reactive (Q) powers of interfacing inverter

The system is now updated with P&O MPPT in the SMC module for optimal control of the boost converters. PV module boost controllers update the P&O MPPT, and a simulation is conducted for the same rating and duration. After the P&O MPPT update the active powers from the PV source are recorded with the updated of AWPI controller in inverter control, the THDs (Total Harmonic Distortions) of the inverter voltage and current are calculated using FFT analysis tool and are presented in Figure 11.

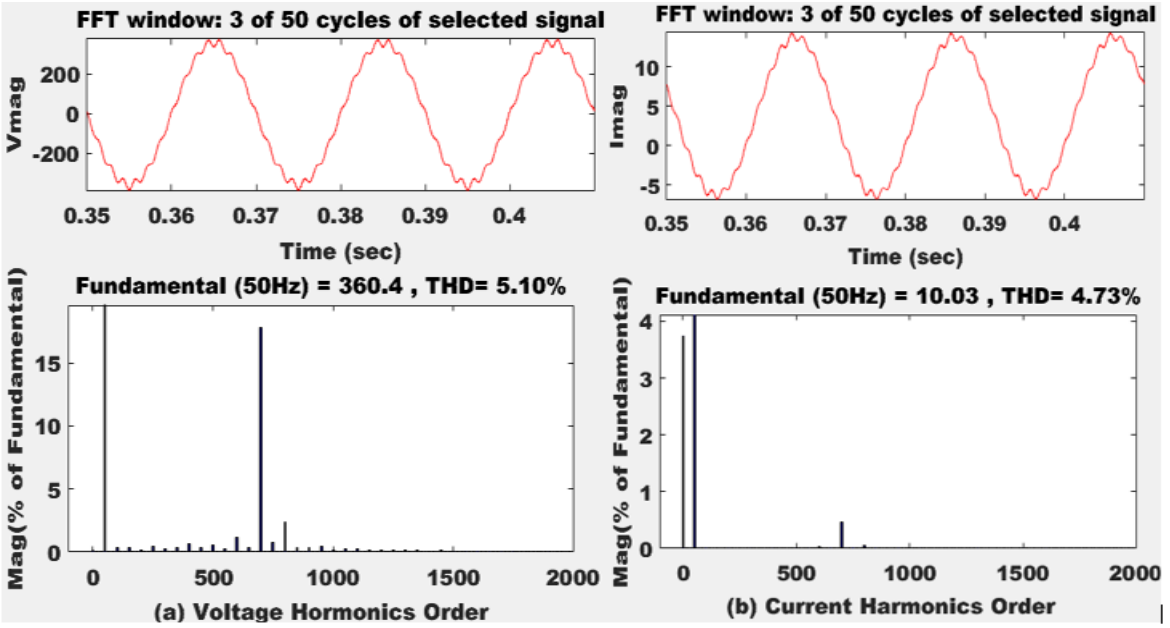

Figure 11: FFT analysis of a) Inverter Voltage and b) Inverter Current with AWPI controller.

As per the calculated THDs of the voltage and current with SMC P&O MPPT values are lower as observed in Figure 11.

VI.CONCLUSION

A standalone renewable energy **system** with a battery energy storage **(**BES) backup module is developed, incorporating advanced maximum power point tracking (MPPT) techniques and active power control **(**APC)-based anti-windup proportional-integral (AWPI) inverter control**.** The photovoltaic (PV) module operates with power extraction converters utilizing the sliding mode control (SMC) perturb and observe (P&O) MPPT technique. This MPPT module ensures stable voltage generation while maximizing power extraction from renewable sources**.** The extracted renewable power is either stored in the battery or supplied to the local load based on demand. The conventional P&O MPPT technique is optimized for efficient power extraction. The maximum power output of the PV module is raised by 14 kW by improving the P&O MPPT algorithm. Additionally, due to improved dq-axis signal stability achieved by the AWPI controller, The inverter greatly reduces the three-phase voltages and currents' total harmonic distortion (THD). The voltage and current THD is reduced 5.10% and 4.73%**.** Further reductions in THD can be achieved by integrating advanced control techniques into the active power control of the inverter**.**

REFERENCES

1. *W. Zhuo, "Control Strategies for Microgrids with Renewable Energy Generation and Battery Energy Storage Systems," arXiv preprint arXiv:1911.02126, Nov. 2019. arxiv.org/abs/1911.02126.*
2. *G. A. Barzegkar-Ntovom et al., "Assessing the viability of Battery Energy Storage Systems coupled with Photovoltaics under a pure self-consumption scheme," Renewable Energy, vol. 152, pp. 1302-1309, Jun. 2020. doi.org/10.1016/j.renene.2020.01.061.*
3. *R. Tonkoski, L. A. C. Lopes, and T. H. M. EL-Fouly, "Coordinated active power curtailment of grid connected PV inverters for overvoltage prevention,"* IEEE Transactions on Sustainable Energy, *vol. 2, no. 2, pp. 139–147, Apr. 2011. doi: 10.1109/TSTE.2010.2103369.*
4. ***M. Forouzesh, Y. P. Siwakoti, S. A. Gorji, F. Blaabjerg, and B. Lehman**, "Step-Up DC–DC Converters: A Comprehensive Review of Voltage-Boosting Techniques, Topologies, and Applications,"* IEEE Transactions on Power Electronics, *vol. 32, no. 12, pp. 9143–9178, Dec. 2017. [Online]. Available: https://doi.org/10.1109/TPEL.2017.2652318.*
5. ***O. N. Almasi, V. Fereshtehpoor, M. H. Khooban, and F. Blaabjerg,** "Analysis, Control and Design of a Non-Inverting Buck-Boost Converter: A Bump-Less Two-Level T–S Fuzzy PI Control,"* ISA Transactions, *vol. 67, pp. 515–527, Mar. 2017. [Online]. Available: https://doi.org/10.1016/j.isatra.2017.01.003.*
6. ***M. Liserre, R. Teodorescu, and F. Blaabjerg,** "Stability of Photovoltaic and Wind Turbine Grid-Connected Inverters for a Large Set of Grid Impedance Values,"* IEEE Transactions on Power Electronics, *vol. 21, no. 1, pp. 263–272, Jan. 2006. [Online]. Available: https://doi.org/10.1109/TPEL.2005.861185.*
7. *Kjaer, S. B., Pedersen, J. K., & Blaabjerg, F. (2005). A Review of Single-Phase Grid-Connected Inverters for Photovoltaic Modules. IEEE Transactions on Industry Applications, 41(5), 1292–1306. doi:10.1109/tia.2005.853371.*
8. ***M. G. Villalva, J. R. Gazoli, and E. Ruppert Filho,** "Comprehensive Approach to Modeling and Simulation of Photovoltaic Arrays,"* IEEE Transactions on Power Electronics, *vol. 24, no. 5, pp. 1198–1208, May 2009. doi.org/10.1109/TPEL.2009.2013862.*
9. ***M. Fadaee and M. A. M. Radzi,** "Multi-Objective Optimization of a Stand-Alone Hybrid Renewable Energy System by Using the Teaching–Learning-Based Optimization Algorithm," IEEE Transactions on Industrial Electronics, vol. 60, no. 4, pp. 1744–1755, Apr. 2013. 10.1016/j.rser.2012.02.071.*
10. *Debnath, D., & Chatterjee, K. (2015). Two-Stage Solar Photovoltaic-Based Stand-Alone Scheme Having Battery as Energy Storage Element for Rural Deployment. IEEE Transactions on Industrial Electronics, 62(7), 4148–4157. doi:10.1109/tie.2014.2379584.*
11. *Patel, H., & Agarwal, V. (2008). Maximum Power Point Tracking Scheme for PV Systems Operating Under Partially Shaded Conditions. IEEE Transactions on Industrial Electronics, 55(4), 1689–1698. doi:10.1109/tie.2008.917118.*
12. ***S. S. Shirsath, A. V. Sutagundar, and R. K. Malagi,** "Sliding Mode Control Based MPPT for a Photovoltaic System Using Boost Converter,"* IEEE International Conference on Power Electronics, Intelligent Control and Energy Systems (ICPEICES), *Delhi, India, pp. 1–5, 2018. [Online]. Available: https://doi.org/10.1109/ICPEICES.2018.8897426.*
13. *Sangwongwanich, A., Yang, Y., & Blaabjerg, F. (2016). High-Performance Constant Power Generation in Grid-Connected PV Systems. IEEE Transactions on Power Electronics, 31(3), 1822–1825. doi:10.1109/tpel.2015.2465151.*
14. *Farias, G. A. B., & Reginatto, R. (2018). Anti-Windup Action in Inverters Control of Distributed Generation Photovoltaic Systems. 2018 13th IEEE International Conference on Industry Applications (INDUSCON). doi:10.1109/induscon.2018.8627307.*
15. ***A. B. Nassim, M. Becherif, M. Abbes, and A. Malek,** "Enhanced Photovoltaic Systems Performance: Anti-Windup PI Controller in ANN-Based ARV MPPT Method," Energy Reports, vol. 6, pp. 697–707, Nov. 2020. DOI: 10.1109/ACCESS.2023.3290316.*